

Electrochemical Behavior of a Stainless Steel Superficially Modified with Nitrogen by Three-dimensional Ion Implantation

Comportamiento electroquímico de un acero inoxidable modificado superficialmente con nitrógeno por medio de implantación iónica tridimensional

Felipe Sanabria-Martínez¹, Ely D. Valbuena-Niño², Leidy S. Chacón-Velasco³, and Hugo A. Estupiñán-Durán⁴

ABSTRACT

Martensitic-grade stainless steels are widely used in diverse industrial and surgical applications, despite their natural tendency to suffer local and uniform corrosion when continuously exposed to aggressive operation conditions. In order to enhance their surface properties, this paper characterized the performance, in saline solutions, of AISI 420 stainless steel, which was surface-modified by three-dimensional ion implantation using electrochemical techniques. The surface of the samples was implanted with ionized nitrogen particles with an energy of 10 keV, varying the implantation time between 30 and 90 minutes. After the surface treatment, the samples were exposed to a NaCl 3% (w/w) aqueous solution for 21 days. Tafel extrapolation, linear polarization resistance, and electrochemical impedance spectroscopy tests were performed, with the purpose of quantifying the effect of the ion implantation technique against electrochemical corrosion. To establish a comparison, the same tests were also performed on non-treated samples. The results indicated an increase in the corrosion potential, polarization resistance, and a decrease in the current density of implanted samples, thus demonstrating that, by delaying corrosive activity, three-dimensional ion implantation offers better protection against electrochemical corrosion in AISI 420 stainless steel samples implanted with nitrogen.

Keywords: martensitic steel, surface, surface modification, corrosion, electrochemical characterization

RESUMEN

Los aceros inoxidables de grado martensítico son ampliamente usados en diversas aplicaciones industriales y quirúrgicas, a pesar de su tendencia natural a presentar corrosión de tipo uniforme y localizada cuando son continuamente expuestos a condiciones de operación agresivas. Con el propósito de mejorar sus propiedades superficiales, este trabajo caracterizó el desempeño en solución salina del acero inoxidable AISI 420 modificado superficialmente por medio de la técnica de implantación iónica tridimensional usando técnicas electroquímicas. La superficie de las probetas fue implantada con partículas ionizadas de nitrógeno a una energía de 10 keV, variando el tiempo de implantación entre 30 y 90 minutos. Posterior al tratamiento superficial, las muestras fueron expuestas a una solución acuosa de NaCl al 3% wt durante 21 días. Se llevaron a cabo pruebas de extrapolación Tafel, resistencia a la polarización lineal y espectroscopía de impedancia electroquímica, con el objetivo de cuantificar el efecto de la técnica de implantación frente a la corrosión electroquímica. Con motivo de establecer una comparación, los mismos ensayos fueron aplicados a muestras sin tratamiento. Los resultados indicaron un aumento en el potencial de corrosión, resistencia a la polarización y una disminución en la densidad de corriente en probetas implantadas, demostrando así que, retardando la actividad corrosiva, la implantación iónica tridimensional ofrece una mejor protección frente a la corrosión electroquímica en sustratos de acero inoxidable AISI 420 implantados con nitrógeno.

Palabras clave: acero martensítico, superficie, modificación superficial, corrosión, caracterización electroquímica

Received: March 18th, 2020

Accepted: June 25th, 2021

¹Chemical Engineer, Universidad Industrial de Santander, Bucaramanga, Colombia. Affiliation: Foundation of Researchers in Science and Technology of Materials, Colombia. E-mail: felipesanabriamartinez@gmail.com

²Physicist, Universidad Industrial de Santander, Bucaramanga, Colombia. Master in Physics, Universidad Industrial de Santander, Bucaramanga, Colombia. Ph.D. in Mechanical Engineer, Universidad Politécnica de Madrid, Madrid, España. Affiliation: Foundation of Researchers in Science and Technology of Materials, Colombia. E-mail: edvnino@foristom.org

³Metallurgical Engineer, Universidad Industrial de Santander, Bucaramanga, Colombia. Affiliation: Foundation of Researchers in Science and Technology of Materials, Colombia. E-mail: leidy silvanacv@hotmail.com

⁴Metallurgical Engineer, Universidad Industrial de Santander, Bucaramanga,

Colombia. Master in Engineering, Universidad Industrial de Santander, Bucaramanga, Colombia. Ph.D. in Chemical Engineering, Universidad Industrial de Santander, Bucaramanga, Colombia. Affiliation: Associate Professor, Universidad Nacional de Colombia, Medellín, Colombia. Email: haestupinand@unal.edu.co

How to cite: Sanabria-Martínez, F., V-Niño, E. D., Chacón-Velasco, L. S., and Estupiñán-Durán, H. A. (2022). Electrochemical Behavior of a Stainless Steel Superficially Modified with Nitrogen by Three-dimensional Ion Implantation. *Ingeniería e Investigación*, 42(1), e85772. 10.15446/ing.investig.v42n1.85772



Attribution 4.0 International (CC BY 4.0) Share - Adapt

Introduction

Grade 420 martensitic stainless steel (AISI 420 SS) is a high carbon steel with a chromium mass content of up to 14% and other alloying elements such as Mn (1%), Mo (1%), Si (1%), S (0,03%), and P (0,04%). This compositional structure, along with its heat treatment during the manufacturing process, makes it an attractive material for various industrial applications in modern engineering; it has a remarkable operational performance in electrolytic environments and relatively important mechanical properties (hardness and ductility). Despite this, grade 420 SS suffers great damage when exposed to certain conditions, for instance, when operating under annealed conditions or at high temperatures. This type of steel has demonstrated a lower corrosion resistance and pitting tendency in comparison with other martensitic and austenitic alloys (Voort *et al.*, 2004).

Due to cases of this type, the enhancement of the physicochemical properties (particularly in structures of metallic nature), by means of novel, safe, and reliable techniques working with easy-to-operate, inexpensive, and ecofriendly equipment designed specifically to advance in the engineering of solid materials and surface technology, has attracted a growing interest by the scientific community. Numerous experiments have shown that the surface properties of metals, altered by phenomena such as friction, wear, fatigue, and corrosion can be changed with superficial modifications by doping species upon the surface of the solid, and they have also uncovered feasible possibilities for improving the functional capability of several alloys in a variety of applications (Borgioli *et al.*, 2019; Bravo and Vieira, 2015; Walsh *et al.*, 2008). Recently, a number of ion bombardment techniques such as direct ion implantation (or ion beam), ion beam assisted deposition, or plasma source ion implantation, among other variations, have been increasingly implemented for surface treatments, exhibiting a potential for producing, in quantitative terms, enhancements in wear and corrosion applications in metals and alloys at several orders of magnitude.

Initially, ion implantation was commercially presented in the semiconductor industry. Then, it happened to be studied at different laboratories across the world, whose works were aimed at the possibility of improving mechanical and corrosion behavior of steels that are of relevance to the nuclear and metallurgical industry (Was, 1990; Dearnaley, 1969; National Research Council, 1979). In general, the impinging atoms penetrate the target or substrate material at a depth between 0,01 and 1,00 μm , which produces a thin alloyed surface layer on the substrate without altering neither the geometric dimensions nor their internal properties. The implantation range of the atoms depends on the atomic number and the energy at which the atom is accelerated. The process differs from others such as electroplating in that it does not produce a discrete coating, as well as from or carburizing and nitriding, which involve diffusion of species at greater depths into the material at high temperatures. Instead, ion implantation alters the chemical composition near the surface of the base material. Within

the phenomena occurred during the surface modification of the solid surface by ion bombardment, both compositional and microstructural changes can be identified, which lead to the alteration of physicochemical properties such as transport, optical properties, corrosion, strength and wear, and fatigue resistance. The compositional changes associated with ion implantation are classified into recoil implantation, cascade mixing, radiation-enhanced diffusion, radiation-induced segregation, Gibssian adsorption, and sputtering, which, combined, produce complex composition differentials upon the implanted surface. Microstructurally, within the formation of defects expected from thermodynamic equilibrium, it is possible to find phase alterations, metastable (crystalline, amorphous, or quasicrystalline) phase formation and growth, grain growth, texture, and the formation of a high-density dislocation network. It is worth noting that, compared to other surface processes, several advantages have been demonstrated for using ion implantation as a surface modification technique:

- The operation is inherently conducted at low temperatures.
- It yields exceptional adhesion.
- Dimensional changes are not a problem on an engineering tolerance scale (being around the order of a few tenths of nanometers).
- Surface polish is enhanced by the sputtering process.
- The implanted species are dispersed on a microscopic-atomic level, thus producing the most efficient and beneficial effect of the additive.
- Significant compressive surface stresses are produced, which compensate external imposed tensile stresses and protect the components against creep or fatigue failure by surface-initiated cracking.

Notwithstanding the above, an important limitation in metallurgical applications has also been found, where a complete and homogeneous implantation of species upon the surface is required. Certain sections of the surface of complex shapes may be inaccessible to the line-of-sight capability of conventional equipment, thus leading to the expensive and bulky installation of sample manipulation devices (Was, 1990; Dearnaley, 1969; National Research Council, 1979). With the purpose of improving the functionality in corrosive environments of ferrous alloys widely used in engineering applications, this paper presents the results obtained from the electrochemical analysis of a 420-grade stainless steel surface modified by three-dimensional ion implantation (3DII), a particular implantation technique that overcomes the limitations mentioned above. By means of 3DII, nitrogen (N) ions are bombarded upon the surface of AISI 420 SS substrates at previously established energy levels and exposition times (Dougar-Zhabon, 1999, 2002; Valbuena-Niño *et al.*, 2010, 2011, 2020; Sanabria *et al.*, 2019, 2020). Then, the effect of the surface modification and performance of the SS samples

exposed to an aggressive media simulating work operation is evaluated through the following electrochemical techniques: linear polarization resistance (LRP), Tafel extrapolation, and electrochemical impedance spectroscopy (EIS).

Methodology

In general, the experimental methodology in this work was sequentially developed as follows: substrate preparation, definition of parameters prior the ion implantation treatment, and electrochemical characterization.

Substrate material

Disk-shaped AISI 420 SS substrate with a 13 mm diameter and 2 mm thickness were used in this study (see chemical composition in Table 1). Before the surface treatment, the metallographic preparation was carried out in accordance with ASTM standards (2003, 2011a). The samples were ground and then polished with silicon carbide papers from 60 down to 600 grit. Additionally, in order to understand the state and phases of the delivered material, a microstructure analysis was performed with a Carl Zeiss JVC metallographic microscope.

Table 1. Elemental composition of AISI 420 SS

Element	C	Cr	Mn	Si	S	P
Value (wt %)	0,30	13,56	0,50	1,00	0,03	0,04

Source: Authors

Ion implantation

3DII is performed by means of the Joint Universal Plasma and Ion TEchnology Reactor (JUPITER), a prototype of this technique. The process is based on a high voltage pulsed discharge activated within the low-pressure range or 'high vacuum'. For a more detailed description of the properties, phenomena, and other generalities occurred in this type of plasma-ion technology, a review of the referenced literature is encouraged (Parada *et al.*, 2019; Vladimir and Tsygankov, 1997). Once the samples are placed upon the cathode (the region where the applied voltage drops) inside the vacuum chamber of the reactor, a pump system is set up to achieve the required vacuum operations and then ignite the discharge. At this pressure conditions, an ion flux of gaseous nitrogen is fed into the chamber. Once exposed to the applied potential (whose magnitude is of an order from tenths to hundredths of kiloelectronvolts), the gas particles reach an ionization state and then, due to the auto-sustained plasma, which is generated by the effect of this type of discharge at such conditions, the excited particles are attracted towards the cathode, also granting the implantation of ionized species upon the surface of the substrates at a normal angle on the surface. Additionally, prior to the implantation process in this study, there was additional surface preparation by sputtering. That is, before feeding in the ion flux of nitrogen, an Argon (Ar) flux was supplied at certain conditions with

the purpose of eliminating the greatest possible amount of impurities and adapting the roughness across the surface of the substrates. The JUPITER operation conditions for both processes (sputtering and ion implantation) agree with previous experiments and shown in Table 2 (Dougar-Zhabon *et al.*, 1999, 2002; Valbuena-Niño *et al.*, 2010, 2011, 2020; Sanabria *et al.*, 2019, 2020).

Table 2. Operation conditions

Parameter	Sputtering	Treatment (T1)	Treatment 2 (T2)
Gas type	Ar	N	N
Voltage (V)	5	30	30
Frequency (Hz)	30	30	30
Pulse duration (ms)	0,25	0,25	0,25
Pressure (Pa)	1,5 > P > 1,8	1,5 > P > 1,8	1,5 > P > 1,8
Exposition time (min)	20	30	90

Source: Authors

Electrochemical characterization

Implanted and non-implanted substrates were immersed in an electrolyte solution with NaCl (wt. 3%) for 21 days, and electrochemical tests were periodically performed on days 0, 7, 14, and 21. To measure the electrochemical corrosion behavior of AISI 420 SS samples, an electrochemical cell with a KCl salt bridge and Agar-Agar solution was implemented. A typical cell consists of three electrodes, in which AISI 420 SS specimen served as the working electrode with an area of 0,785 cm², a graphite rod as the counter electrode, and Ag/AgCl (saturated calomel electrode) as the reference electrode. This cell is then connected to Gill B1-STAT through a potentiostat plugged into a computer with the ACM v.5 software and a sequencer, as mentioned in the G106-89 standard (ASTM, 2015).

It is worth noting that all electrochemical and corrosion tests were performed according with ASTM standards (2010, 2011b). The Tafel extrapolation test was performed with a scan rate of 1 mV/sec and a potential between -250 mV and +250 mV. LPR analysis was carried out with a linear fit between +25 mV and -25 mV around the previously established corrosion potential (E_{corr}). As for the electrochemical impedance measurements, the spectrums were recorded with an initial and final frequency of 30 000 Hz and 0,05 Hz, respectively. The impedance response was eventually obtained from the applied frequency range and then analyzed by Nyquist plots and Bode representation. An equivalent circuit was proposed to physically interpret the obtained data from EIS measurements. The procedures mentioned above were followed to determine the kinetic parameters (E_{corr}), corrosion current density (i_{corr}), and polarization resistance (R_p). Additionally, the experimental data were simulated by running different types of electrode-electrolyte interfaces with the Zview software (Scribner Associates, Inc.), thus finding the best electric circuit representation, accurately describing each electrochemical

system, and determining the respective values of each component involved.

Results

The characterization results before and after the implantation process are presented in this section in the following way: a metallographic analysis, an electrochemical study with potentiodynamic analysis (Tafel and LPR), and EIS measurements.

Metallographic analysis

The micrograph of the structure is illustrated in Figure 1, which agrees with the typical microstructure of the martensitic stainless steel (AISI 420 SS) supplied in annealed conditions. It consists mainly of ferrite, together with perlite grains dispersed with small colonies of carbides precipitated at the grain boundaries (Nunura and Lecaros, 2015; Voort *et al.*, 2004).

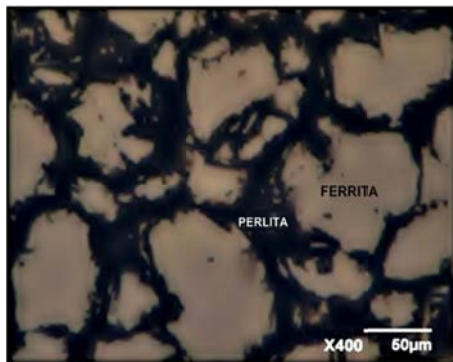


Figure 1. Metallography structure: AISI 420 SS.

Source: Authors

Electrochemical analysis

Extrapolation Tafel: In order to obtain information concerning the corrosion resistance of AISI 420 SS, the quantitative assessment of corrosion was conducted by potentiodynamic polarization tests. Figure 2 illustrates the comparison of the potentiodynamic polarization curves between implanted and non-implanted samples exposed to NaCl (wt. 3%) solution at different exposition times. The relevant parameters are listed in Table 3.

From the Tafel analysis, the E_{corr} value gives an idea of the reactive nature of the surface of AISI 420 SS. In general terms, it can be noticed that, during each stage of the experiment, the blanks, compared with implanted samples, described an active corrosion tendency with a more negative E_{corr} and a rapid increase in the anodic reaction rate. As a result, a more important deterioration of corrosion resistance may be expected. Regarding the implanted samples, the E_{corr} values shifted towards nobler sides, where the samples that stood out were those whose nitrogen ion implantation was carried out for 90 minutes and exposed at 0, 7, and 21 days. Unlike the latter, at 14 days, it was found that the E_{corr} value for

the substrates implanted for 30 minutes was slightly higher, which did not allow establishing a linear correlation between E_{corr} and treatment time during ion implantation with nitrogen on AISI 420 SS. Nevertheless, the analysis of the corrosion potential is only a first approximation of the electrochemical behavior of the material, and other parameters like i_{corr} must be taken into account in order to evaluate corrosion kinetics.

Corrosion current density (i_{corr}) was estimated by means of linear fit and Tafel extrapolation to the cathodic part of the polarization curve. From Table 3, it can be observed that the corrosion current density (i_{corr}) is inversely proportional to the corrosion potential (E_{corr}), which implies the same pattern of corrosion behavior, that is, an increase in i_{corr} implies a degradation of the protective properties of the passive film formed during the implantation process. As mentioned before, the reaction rate in samples without treatment remained the highest throughout the exposition time in saline solutions. Conversely, it can be observed that the E_{corr} and i_{corr} of the implanted samples provided better results compared to non-implanted samples. Since the i_{corr} magnitudes reflect the rate of dissolution through the passive layer, it can be concluded that the samples implanted with nitrogen for 30 minutes possess a better corrosion resistance in comparison with the blanks. Thus, it can be said that the treatment with the same ion implanted for 90 minutes exhibits the highest corrosion resistance. As for the inspection at 14 days of chemical attack, the samples implanted for 90 minutes showed an increase in E_{corr} accompanied by lower i_{corr} than those implanted for 30 minutes, which confirms a more important improvement in the corrosion resistance of AISI implanted with nitrogen under these conditions. Finally, it is worth mentioning the existence of a transpassive region, where the rapid increase in the current value occurs due to a breakdown of the passive films. This tendency is commonly known as pitting corrosion, and it is made evident in Figure 2c for the samples implanted for 30 minutes at a potential of 0,06 V. A more notable tendency of this phenomena is presented in Figure 2d for blanks and samples implanted for 90 minutes at potentials of 0,06 V and 0,12 V, respectively. (Anandan *et al.*, 2007; Maleki-Ghaleh *et al.*, 2014; Muthukumaran *et al.*, 2010; Padhy *et al.*, 2010; Pereira *et al.*, 2017; Osozawa and Okato, 1976).

Table 3. Electrochemical parameters obtained from Tafel analysis

Substrates	Parameter	0 days	7 days	14 days	21 days
Blanks	E_{corr} (V)	-573,90	-543,60	-530,00	-164,00
	i_{corr} (A/cm ²)	3,16E00	2,51E00	2,95E00	3,55E-01
T1 (30 min)	E_{corr} (V)	-524,50	-371,70	-163,70	-128,90
	i_{corr} (A/cm ²)	2,51E00	6,31E-01	3,98E-01	6,31E-02
T2 (90 min)	E_{corr} (V)	-355,80	-348,70	-183,20	-104,00
	i_{corr} (A/cm ²)	1,78E+00	6,31E-01	5,89E-02	2,00E-02

Source: Authors

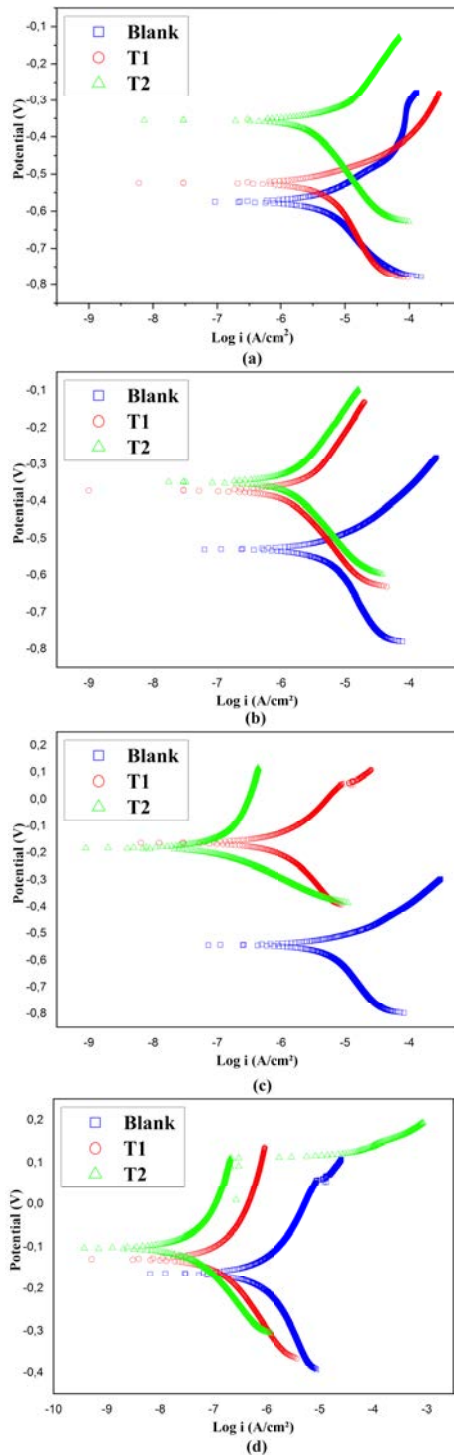


Figure 2. Potentiodynamic curves: Samples exposed to NaCl (wt. 3%) at (a) 0 days, (b) 7 days, (c) 14 days, and (d) 21 days.

Source: Authors

Several works have attributed the beneficial effect of nitrogen ion implantation in ferrous alloys to different physical and chemical phenomena such as the supersaturation of the atomic structure, the generated stresses, and the defect density (Sanabria *et al.*, 2020). Regarding the electrochemical properties of stainless steels, the contribution of both implanted nitrogen and the formation of chromium nitride

on the metal's surface have been confirmed as the main mechanisms in the enhancement of corrosion potential and current density. On one hand, the decrease in i_{corr} is attributed to the formation of stable chromium nitride phases inside the interstitial sites, which act as a kinetic barrier to the dissolution process of the alloy, hence reducing the reaction rate due to a multi-electron transfer process.

Other authors (Anandan *et al.*, 2007; Muthukumaran *et al.*, 2010; Padhy *et al.*, 2010) have proposed a different approach to the effect of implanted nitrogen on electrochemical behavior. Implanted nitrogen favors the formation of ammonium ions (Equation (1)) which eventually increase the local pH at active sites on the surface, such as grain boundaries and kinks, where passive film formation is chiefly unstable. As a result, the production of ammonium, together with further nitrite or nitrate ions through the electrolyte, impedes the reduction of pH, thus shifting the E_{corr} to more positive values (Fossati *et al.*, 2006).



Linear polarization resistance: Linear polarization resistance is inversely related to the corrosion rate and provides useful information on the reactivity of AISI 420 SS in electrolytes. The knowledge of R_p from the cathodic zone enables the direct determination of i_{corr} and, hence, the corrosion rate at any instant (Vasilescu *et al.*, 2015). The results obtained after the exposition to a NaCl (wt. 3%) solution while performing the linear polarization test in non-implanted and implanted samples are presented by the graphs in Figure 3.

The relation between the potential and the current density of non-implanted samples is depicted in Figure 3a. The typical trend of polarization curves was observed, with a relatively similar R_p values at 0 days (3 364,2 $\Omega \cdot \text{cm}^2$), 7 days (3 632,8 $\Omega \cdot \text{cm}^2$), and 14 days (3 937,6 $\Omega \cdot \text{cm}^2$). It then reached the highest value at 21 days (12 810,0 $\Omega \cdot \text{cm}^2$) of exposition due to a possible passivation of the metallic surface by the formation of a chrome oxide film, a natural characteristic of martensitic SS against corrosion. As for the results in the current-potential profile of implanted samples, a remarkable difference between the R_p values was observed; there was a gradual magnitude increase during the immersion time in the saline solution. In the case of the substrates implanted with nitrogen for 30 minutes in Figure 3b, the R_p values were 2 812,1 $\Omega \cdot \text{cm}^2$, 19 562,0 $\Omega \cdot \text{cm}^2$, and 36 455,0 $\Omega \cdot \text{cm}^2$ at 0, 7, and 14 days, respectively. At 21 days, where the R_p reached the highest magnitude or polarization resistance (248 905,0 $\Omega \cdot \text{cm}^2$), the curve presented a vertical trend of quasi-steady current as the potential increased, which indicates the formation of a passive film upon the surface. Similarly, the samples implanted with nitrogen for 90 minutes (Figure 3c) exhibited such tendency, where the R_p values at 0 and 7 days were 6 553,3 $\Omega \cdot \text{cm}^2$ and 28 030,0 $\Omega \cdot \text{cm}^2$, respectively. However, this system achieved the passive behavior at 14 days with an R_p of 269 228,0 $\Omega \cdot \text{cm}^2$, and then at 21 days with the highest polarization resistance at 812 510,0 $\Omega \cdot \text{cm}^2$. An overall R_p behavior of the samples is shown in Figure 3d.

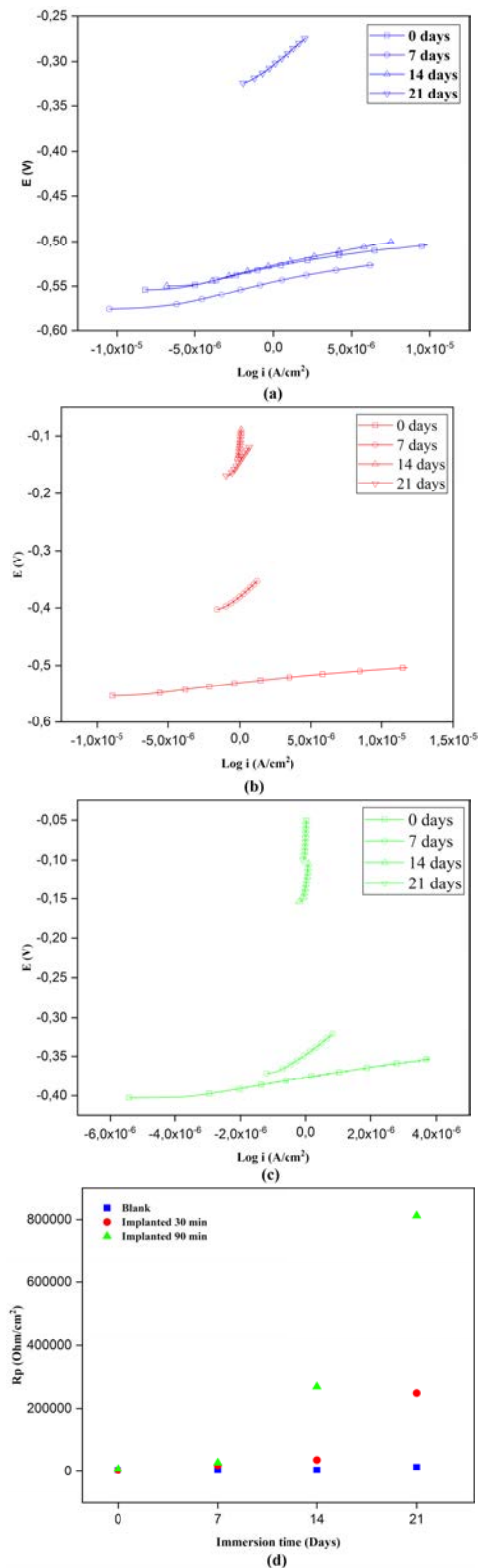


Figure 3. Linear polarization resistance plots: $\text{Log } i$ (current density) vs. Potential (v) plots of non-implanted (a) and implanted with nitrogen for (b) 30 minutes, (c) 90 minutes, and (d) R_p vs. exposition time in NaCl. **Source:** Authors

By means of this electrochemical measurement, a favorable effect of 3DII technique with nitrogen species upon the surface of martensitic stainless steels was demonstrated; it gradually reduced the current flux across the substrate surface and therefore boosted its corrosion resistance during the immersion time in the electrolyte solution. Additionally, a linear correlation was established between the R_p and treatment time, with a better protection at relatively longer times of nitrogen ion implantation. A reason for this is that the surface of implanted substrates effectively achieves a passive behavior due to the formation of a stable and protective surface oxide layer. This delays the effect of anodic reactions upon the surface of the material once exposed to the chemical attack. Other 3DII studies have found a direct correlation between the treatment time and the implantation dose, reporting better corrosive behavior at higher doses due to the effect of the concentration of the implanted species (Valbuena-Niño *et al.*, 2020; Sanabria *et al.*, 2019). The findings in the LPR measurements agree with other works (Valbuena-Niño *et al.*, 2011; Peña *et al.*, 2009) and reinforce the results obtained in the Tafel analysis regarding the electrochemical behavior of AISI 420 SS against electrochemical corrosion.

Electrochemical Impedance Spectroscopy: Whereas potentiodynamic polarization analysis can give information about the susceptibility of the surface to corrosion, EIS experiments can provide more data concerning to the corrosion mechanisms.

The evolution of the electrochemical behavior of non-implanted AISI 420 SS samples and samples surface-treated by nitrogen ion implantation for 30 and 90 minutes, then exposed to a saline environment for 0, 7, 14, and 21 days, is indicated by the common EIS representations: Nyquist plots and Bode diagrams. Additionally, an appropriate equivalent circuit with its corresponding fitted parameters, such as constant phase elements (CPE), solution resistance (R_s), pore resistance (R_L), and R_p , is also presented in Table 4 and described in a section below.

In Figure 4, the Nyquist plots are illustrated from EIS measurements carried out at different exposition times for both non-implanted (Figure 4a) and implanted samples with nitrogen species at different treatment times (Figure 4b and c). All the Nyquist plots end up with an unfinished semicircular form. A similar electrochemical tendency can be seen in the implanted samples, where the influence of 3DII with nitrogen particles is made evident by comparing the radius of the curves with those described by the blanks. The difference lies in the shifting of the curves for the implanted samples along the real axis, which is due to the series resistances comprising electrolytes and contact resistance. This can be validated from the values obtained in Table 4. Since high R_p values suggest a good corrosion resistance, and low capacitance magnitudes signify the long-term stability of the passive film, the geometric increment in the curve amplitudes is attributed to a direct increase between the polarization resistances of each system with both the exposition time and treatment time in the implantation process. The R_p increased from 990,0 $\Omega \cdot \text{cm}^2$ (0 days) to 22 516,0 $\Omega \cdot \text{cm}^2$ (21 days) in blanks (Figure 4a), from 842,7 $\Omega \cdot \text{cm}^2$ (0 days) to 26 000,0 $\Omega \cdot \text{cm}^2$

(21 days) in samples implanted for 30 minutes (Figure 4b), and from $5\,557,0\ \Omega\cdot\text{cm}^2$ (0 days) to $463\,780,0\ \Omega\cdot\text{cm}^2$ (21 days) in samples implanted for 90 minutes (Figure 4c).

Conversely, the double layer capacitance for each system globally presented a reduction in its magnitude throughout the electrochemical exposition from $9,38\text{E-}03\ \text{F}\cdot\text{cm}^{-2}$ to $9,70\text{E-}06\ \text{F}\cdot\text{cm}^{-2}$ in blanks (Figure 4a); from $2,64\text{E-}3\ \text{F}\cdot\text{cm}^{-2}$ to $6,59\text{E-}06\ \text{F}\cdot\text{cm}^{-2}$ in samples implanted for 30 minutes (Figure 4); and from $3,39\text{E-}04\ \text{F}\cdot\text{cm}^{-2}$ to $8,59\text{E-}06\ \text{F}\cdot\text{cm}^{-2}$ in samples implanted for 90 minutes (Figure 4c). The increase observed in the R_p values in implanted samples is due to stable and readily passive film formation owing to the interfacial nitrogen and the production of chromium nitride. The similar tendency observed in bare substrates, although at a lower degree, may be attributed to the passive nature of martensitic AISI 420 SS in chloride media. As for the capacitance decrease, it indicates an improvement in the passive film stability, thus validating the positive effect on samples implanted with nitrogen (Leitao *et al.*, 1997; Hannani, and Kermiche, 1998).

Figure 5 shows the Bode diagram representation of EIS measurements for blanks and nitrogen implanted on AISI 420 SS samples after immersion in the same corrosive medium. An ideal capacitive response would result in a (-1) slope and a phase angle of 90° . Although no electrochemical system behaves in such an ideal manner, it is possible to identify the expected capacitive behavior of passive films exposed to electrochemical attack in non-implanted samples, a consequence commonly attributed to the characteristic chromium oxide film AISI 420 SS (Hannani and Kermiche, 1998).

Within the exposition time in saline environments, these curves demonstrated a CPE only. A more complex corrosion mechanism was also detected, with alterations in the responses produced by the 3DII technique in surface-modified substrates. Each variation depends on the treatment time during the implantation process and the immersion time in the electrolyte. At high frequencies, there was a significant increase in the phase angle for implanted samples compared to the blanks at 7 (Figure 5b) and 14 days (Figure 5c). However, these findings were contradictory at 0 (Figure 5a) and 21 days (Figure 5d). At low frequencies, implanted samples achieved higher angle phases throughout the immersion period. As for substrates implanted for 90 minutes, a further CPE could be identified within the same exposition time, a typical response from an electrode with a passive layer (Abreu *et al.*, 2008).

Additionally, while the immersion time increases, an improvement can be seen in the ability to resist the current flow with the impedance modulus for implanted samples at low frequencies with higher resistance values than those of blanks. Despite the improvement in electrochemical properties revealed in previous electrochemical techniques, these EIS results suggested that treatment time variations for 3DII with nitrogen species on AISI 420 SS were not able to reproduce a consistent enhancement against corrosion. They were nevertheless considered to give a satisfactory physical interpretation when modeling the corresponding electric circuit.

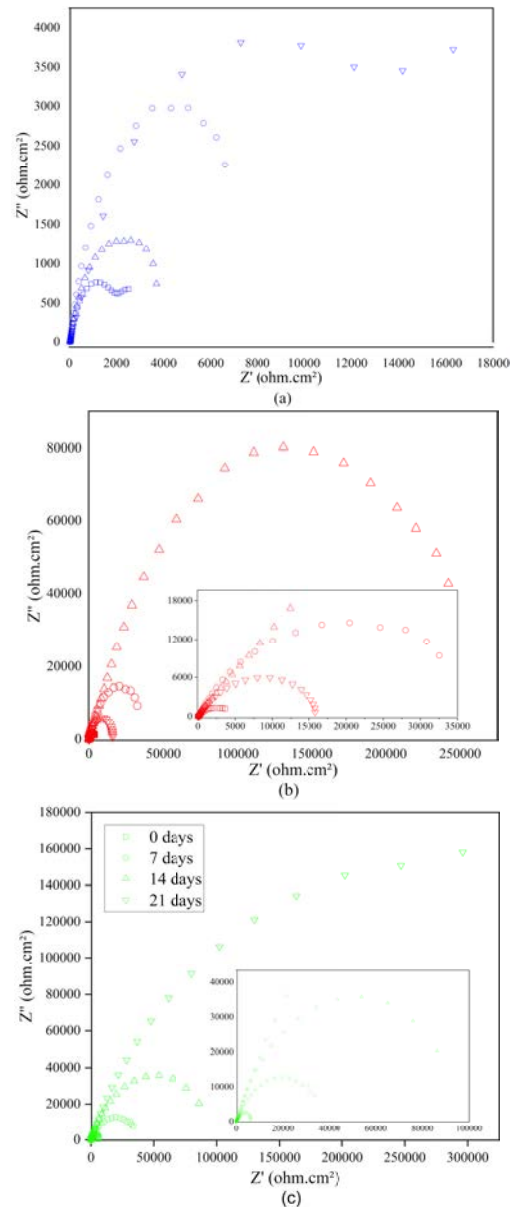


Figure 4. Nyquist diagrams for (a) non-implanted and implanted with nitrogen for (b) 30 minutes and (c) 90 minutes.

Source: Authors

Equivalent circuit: Each system was characterized by using an appropriate equivalent circuit model. The circuit depicted in Figure 6a represents the samples without treatment and can be considered as a simple Randle's cell with only one electroactive interface. The electrical circuit in Figure 6b with two electroactive interfaces is widely used in studies on ion selective membranes (or coated electrode-electrolyte interfaces) when examining metallic corrosion under coatings exposed to corrosive environments (Olaya *et al.*, 2011; Piratoba *et al.*, 2010; Abdi and Savaloni, 2017; Jiménez-Morales *et al.*, 1997).

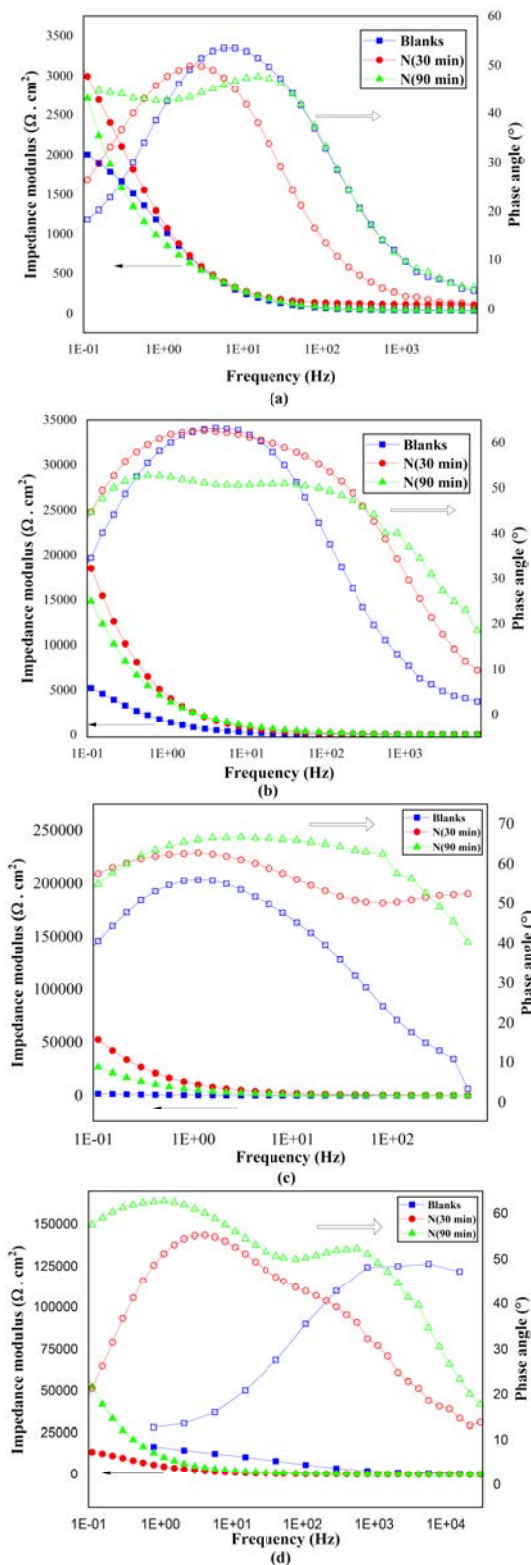


Figure 5. Bode plots for non-implanted and implanted samples after exposition for (a) 0, (b) 7, (c) 14, and (d) 21 days.

Source: Authors

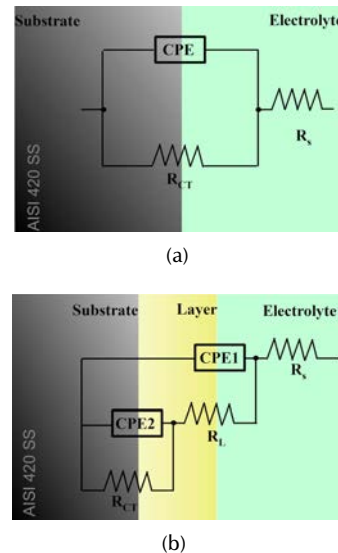


Figure 6. Equivalent circuit representation.

Source: Authors

In general terms, the best electric circuit that fits the experimental data of implanted samples consisted of an arrangement of resistances and pseudo-capacitances or constant phase elements CPE connected in series or parallel. R_s represents the resistance of the solution, for the ion migration describes an ohmic behavior in the electrolyte. The dielectric CPE1 describes the capacitive effect of the interface between the electrolyte and the implanted surface. The following elements correspond to defects or porosities of the passive layer, which ease the transport of the electrolyte, together with oxygen, active ions, and corrosion products, to the metal's surface (Piratoba *et al.*, 2010). The electrolyte precipitated in such an active place is represented by R_L . The electrolyte-substrate interface is represented by the parallel circuit between the dielectric properties of the layer CPE2 (acting as the double layer capacitance), and R_{CT} as the charge transference resistance and the response against polarization resistance. Since CPE accounts for the deviation from an ideal dielectric behavior and is also related to surface heterogeneities, and R_{CT} values give a more approximate interpretation of the corrosion resistance, it is therefore demonstrated that 3DII, applied to this particular material during certain intervals of time, has affected its electrochemical characteristics, and hence its performance in such environments. The fitting parameters were estimated with the Zview software and are shown in Table 4.

Each system increased its R_p and, therefore, the resistance to charge transference at each stage of the chemical exposition. Inversely, a decrease in CPE indicated that the protective layer is either continuous or compact, with the implanted samples being the ones that offered a better improvement in comparison with bare AISI 420 SS substrates. By comparing the performance of implanted samples (with the treatment for 90 minutes standing out) it is possible to conclude that 3DII, for longer periods of time, provides a larger thickness and density of the passive film formed, which, when exposed to chemical attacks, may act as a barrier or blockage of

Table 4. Component values of the equivalent circuit approximation

Substrate	Exposition time in NaCl	R_S ($\Omega \cdot \text{cm}^2$)	R_L ($\Omega \cdot \text{cm}^2$)	R_{CT} ($\Omega \cdot \text{cm}^2$)	CPE1 (F.cm ⁻²)	n1	CPE2 (F.cm ⁻²)	n2
Blank	0	42,0	-	990,0	1,86E-04	0,99	-	-
	7	34,3	-	3 986,0	4,31E-04	0,70	-	-
	14	34,3	-	8 764,0	3,86E-05	0,71	-	-
	21	130,6	-	22 516,0	4,97E-07	0,34	-	-
T1 30 min	0	117,1	-	842,7	2,00E-04	0,75	-	-
	7	58,8	-	16 824,0	2,76E-05	0,69	-	-
	14	35,2	2 191,0	40211,0	4,55E-05	0,75	9,19E-06	0,81
	21	33,1	8 448,0	2,6E+05	3,91E-06	0,77	6,59E-06	0,64
T2 90 min	0	45,6	1 407,0	5 557,0	1,74E-04	0,72	3,39E-04	0,89
	7	33,5	6 190,0	36 392,0	5,79E-05	0,64	1,54E-05	0,92
	14	31,3	122,8	104 700,0	6,64E-06	0,77	7,42E-07	0,76
	21	34,8	2 230,0	463 780,0	1,47E-05	0,70	8,59E-06	0,77

Source: Authors

the active sites of such ferrous alloys. Unexpectedly, some discrepancies were obtained in Bode for samples implanted for 30 minutes at 0 and 7 days of exposition (Figure 5a and b). The curve demonstrated an image similar to non-implanted samples, with one CPE only. This particular case is physically interpreted by means of a Randle circuit (order 1) (Figure 6a), which compromises the following: the resistance offered by the solution, a capacitance that represents the interface electrolyte-substrate, and the charge transference resistance representing the base material. The identical behavior may be attributed to the fact that, at relatively short periods of implantation time, the layer deposited upon the surface of the substrates will not be as stable as those implanted with higher doses or for longer periods, thus offering little protection against electrochemical corrosion (Valbuena-Niño *et al.*, 2016; Sanabria *et al.*, 2019).

The improvement represented by these values is consistent with the findings in the potentiodynamic polarization experiments. The EIS results also provide an additional support to the effect produced by 3DII as a surface modification technique in metal alloys. However, it is unmistakably difficult to determine which physicochemical mechanism activates in order to reduce the corrosive activity. Some authors have observed that nitrogen ion implantation in stainless steels leads to the formation of chromium nitride layers, thus improving the corrosion-resistant of the metal. Moreover, the neutralizing reaction in Equation (1) occurred upon the AISI 420 SS surface implanted with nitrogen in contact with the electrolyte can minimize reaction rates. Other works reported that the increase in defect density generated by the expansion of the lattice would reduce localized corrosion. Finally, the beneficial response of the radiation damage of certain materials exposed to ion implantation was more evident than the chemical effect itself (Muthukumar *et al.*, 2010; Anandan *et al.*, 2007; Padhy *et al.*, 2010; Pereira *et al.*, 2017; Maleki-Ghaleh *et al.*, 2014; Fossati *et al.*, 2006).

Conclusions

The effect of 3DII as a surface modification technique on ferrous alloys was demonstrated through potentiodynamic analysis and EIS measurements. The nitrogen ion implantation applied on AISI 420 SS elements for a duration of 30 minutes and 90 minutes, and then exposed to a saline environment, demonstrated the following:

An improvement in the kinetic parameters was obtained from potentiodynamic analysis. It was determined that substrates implanted under such conditions increased the corrosion potential to nobler values and reduced the reaction rates. Remarkably, the corrosion current density values exhibited a direct correlation with the implantation time. Samples implanted for 30 minutes offered better corrosion properties than blanks. Likewise, samples implanted for 90 minutes offered the best protective properties against electrochemical attacks.

Following this comparison, the reactivity of the material in question was also evaluated through linear polarization resistance. These results validated the findings of the Tafel analysis by identifying the same linear tendency between the R_p and the treatment time. Due to a thicker film formed at higher implantation times, it was possible to obtain higher resistance values, thus delaying the charge transference or current density and then increasing corrosion resistance.

Despite the multilevel variation in the Bode diagrams, a better comparison could be observed in the Nyquist representations and the proposed equivalent circuits. A similar tendency was observed for both implanted and non-implanted samples. However, the resistance and capacitance magnitudes of the samples implanted for 90 minutes showed the best performance against electrochemical corrosion.

The general corrosion behavior demonstrated a significant enhancement after 3DII with the increase in treatment duration and/or implanted dose, thus producing thicker interfaces on AISI 420 SS and enhancing its protective properties against electrochemical corrosion.

Acknowledgements

This research work was supported by the laboratory of “Física y Tecnología del Plasma y Corrosión” and “Grupo de Investigaciones en Corrosión” from the “Universidad Industrial de Santander”. This work was partially financed by the Colombian agency Colciencias through doctoral scholarship 617.

References

- Abdi, F. and Savaloni, H. (2017). Surface nanostructure modification of Al substrates by N⁺ ion implantation and their corrosion inhibition. *Transactions of Nonferrous Metals Society of China*, 27(3), 701-710. 10.1016/S1003-6326(17)60078-5
- Abreu C. M., Cristóbal M. J., Merino P., Novoa X. R., Pena G., and Pérez M.C. (2008). Electrochemical behaviour of an AISI 304L stainless steel implanted with nitrogen. *Electrochimica Acta*, 53(20), 6000-6007. 10.1016/j.electacta.2008.03.064
- Anandan, C., William, V. L., Ezhil, S., and Rajam, K. S. (2007). Electrochemical studies of stainless steel implanted with nitrogen and oxygen by plasma immersion ion implantation. *Surface and Coatings Technology*, 201(18), 7873-7879. 10.1016/j.surfcoat.2007.03.034
- ASTM (2003). *G1-03 Standard practice for preparing, cleaning, and evaluating corrosion test specimens*. ASTM. 10.1520/G0001-03
- ASTM (2010). *G102-89 Standard practice for calculation of corrosion rates and related information from electrochemical measurements*. ASTM. 10.1520/G0102-89R10
- ASTM (2011a). *E3-11 Standard guide for preparation of metallographic specimens*. ASTM. 10.1520/E0003-11
- ASTM (2011b). *G5-94 Standard reference test method for making potentiostatic and potentiodynamic anodic polarization measurements*. ASTM. 10.1520/G0005-94R11E01
- ASTM (2015). *G106-89 Standard practice for verification of algorithm and equipment for electrochemical impedance measurements*. ASTM. 10.1520/G0106-89R15
- Borgioli, F., Galvanetto, E., and Bacci, T. (2019). Surface modification of austenitic stainless steel by means of low pressure glow-discharge treatments with nitrogen. *Coatings*, 9(10), 604. 10.3390/coatings9100604
- Bravo, E. and Vieira I. (2015). Influence of cerium ions and shelf-life of hybrid solution as pre-treatment for AA 2024 aluminium alloy on its anticorrosion performance. *Surface and Interface Analysis*, 48(8), 809-817. 10.1002/sia.5901
- Dearnaley, G. (1969). Ion Bombardment and implantation. *Reports on Progress in Physics*, 32(2), 405-491. 10.1088/0034-4885/32/2/301
- Dugar-Zhabon, V. D., Castro, B. J., Dulce Moreno, H. J., and Tsygankov P. A. (1999). Device JUPITER for ion implantation. *Revista Colombiana de Física*, 31(2), 181-184.
- Dugar-Zhabon, V. D., Dulce Moreno, J., and Tsygankov, P. A. (2002). High voltage pulse discharge for ion treatment of metals. *Review of Scientific Instruments*, 73, 828. 10.1063/1.1429785
- Fossati A., Borgioli, F., Galvanetto, E., and Bacci, T. (2006). Glow-discharge nitriding of AISI 316L austenitic stainless steel: influence of treatment time. *Surface & Coatings Technology*, 200(11), 3511-3517. 10.1016/j.surfcoat.2004.10.122
- Hannani, A. and Kermiche, F. (1998). The Electrochemical Behaviour of AISI 304 Stainless Steel Following Surface Modification by Ion Implantation. *Transactions of the IMF*, 76(3), 114-116, 10.1080/00202967.1998.11871208
- Jiménez-Morales, A., Galván J. C., Rodríguez R., and de Damborenea J. J. (1997). Electrochemical study of the corrosion behaviour of copper surfaces modified by nitrogen ion implantation. *Journal of Applied Electrochemistry*, 27, 550-557. 10.1023/A:1018446628256
- Leitao, E., Silva, R. A., and Barbosa, M. A. (1997). Electrochemical impedance spectroscopy of nitrogen- and carbon-sputter coated 316 L stainless steel. *Corrosion Science*, 39, 333-338. 10.1016/S0010-938X(97)83349-5
- Maleki-Ghaleh, J., Khalil-Allafi, M., Sadeghpour-Motlagh, M. S., Shakeri, S. Masoudfar, A. Farrokhi, Y. Beygi Khosrowshahi, A. Nadernezhad. M. H. Siadati, M.H., Javidi, M., and Shakiba, M. (2014). Effect of surface modification by nitrogen ion implantation on the electrochemical and cellular behaviors of super-elastic NiTi shape memory alloy. *Journal of Materials Science: Materials in Medicine*, 25(12), 2605-2617, 10.1007/s10856-014-5283-4
- Martínez-Orellana L., Pérez, F., and Gómez, C. (2005). The effect of nitrogen ion implantation on the corrosion behaviour of stainless steels in chloride media. *Surface and Coatings Technology*, 200(5-6), 1609-1615. 10.1016/j.surfcoat.2005.08.034
- Muthukumar, V., Selladura, V., Nandhakumar, S., and Senthilkumar, M. (2010). Experimental investigation on corrosion and hardness of ion implanted AISI 316L stainless steel. *Materials and Design*, 31(6), 2813-2817. 10.1016/j.matdes.2010.01.007
- National Research Council (1979). *Ion implantation as a new surface treatment technology*. The National Academies Press. 10.17226/19823
- Nunura, C. and Lecaros, C. (2015). Caracterización del acero inoxidable AISI 420 y los efectos de la presencia de carburos de cromo en la estructura martensítica. *Revista I+i, Investigación Aplicada e Innovación*, 9, 1-10. <https://www.tecsup.edu.pe/sites/default/files/page/file/revista/Volumen-9/Art-1.pdf>
- Olaya, J. J., Piratoba, U., and Rodil S. E. (2011). Resistencia a la corrosión de recubrimientos de CRN depositados por PVD con UBM: tecnología eficiente y ambientalmente limpia. *Revista Latinoamericana de Metalurgia y Materiales*, 31(1), 44-51. <https://www.rlmm.org/ojs/index.php/rlmm/article/viewFile/132/101>

- Padhy, N., Ningshen, S., Panigrahi, B. K., and Kamachi M. (2010). Corrosion behaviour of nitrogen ion implanted AISI type 304L stainless steel in nitric acid medium. *Corrosion Science*, 52(1), 104-112. 10.1016/j.corsci.2009.08.042
- Parada, F. F., Tsygankov P., Dougar-Zhabon, V., Peña, D., Coronado, J., Gonzales, J., and Valbuena-Niño E. D. (2019). Morphologic evaluation of silicon surface modified with titanium and titanium+nitrogen. *Acta Microscopica*, 28(2), 39-47. <https://acta-microscopica.org/acta/article/view/529>
- Peña D., Fontalvo P., Estupiñán H., Valbuena-Niño, E.D., and Vesga W. 2009. Evaluación experimental de la resistencia a la corrosión de un acero AISI-SAE 4140 implantado con iones de nitrógeno. *Dyna*, 76(159), 43-52. <https://revistas.unal.edu.co/index.php/dyna/article/view/13039>
- Pereira C., De Souza, F. S., Marin, G., Hickel, S. M., Bindera C., and Nelmo A. (2017). Corrosion resistance of low-carbon steel modified by plasma nitriding and diamond-like carbon. *Diamond & Related Materials*, 80, 54-161. 10.1016/j.diamond.2017.11.001
- Piratoba, U., Camargo, A., and Olaya J. J. (2010). Impedancia Electroquímica - Interpretación de diagramas típicos con circuitos equivalentes. *Dyna*, 77(164), 6975. <https://revistas.unal.edu.co/index.php/dyna/article/view/25578>
- Sanabria, F., Viejo, F., and Valbuena-Niño, E. D. (2019). Performance in saline environment of a carbon steel surface modified by three-dimensional ion implantation. *Journal of Physics: Conference Series*, 1403, 012015. 10.1088/1742-6596/1403/1/012015
- Sanabria, F., Valbuena-Niño, E. D., Rincón, M., Estupiñán, H. A., and Viejo, F. (2020). Surface evaluation of carbon steel doped with nitrogen ions. *Revista UIS Ingenierías*, 19(1), 205-212. 10.18273/revuin.v19n1-2020019
- Sanabria, F., Gil, L., Matos, C., and Valbuena-Niño E.D. (2019). Experimental evaluation on electrochemical corrosion of ion implanted medium carbon steel of titanium and titanium+nitrogen. *Acta microscopica*, 28(2), 72-85.
- Valbuena-Niño, E. D., Dulce, H. J., and Dugar-Zhabon, V. (2010). Characterization of AISI 4140 Steel Implanted by Nitrogen Ions. *Revista Colombiana de Física*, 42(3), 387-392. <http://revcolfis.org/ojs/index.php/rcf/article/view/420329.html>
- Valbuena-Niño, E. D., Dugar-Zhabon, V., Dulce Moreno, H. J., Peña Rodríguez, G., Garnica, H. A., and Tsygankov, P. (2012). Application of electric arc and high voltage simultaneous discharges for advanced superficial treatment of metals. *Revista Iteckne*, 9(1), 14-20.
- Valbuena-Niño E. D., Gil L., Hernández L., Barba-Ortega J. J., and Dougar-Zhabon V. (2016). Characterization of the alloy steel modified superficially with ions of titanium and nitrogen. *CT&F - Ciencia, Tecnología y Futuro*, 6(3), 135-146. 10.29047/01225383.14
- Valbuena-Niño, E. D., Gil, L., Hernández, L., and Sanabria, F. (2020). Corrosion resistance of a carbon-steel surface modified by three-dimensional ion implantation and electric arc. *Advances in Materials Research*, 9(1), 1-14. 10.12989/amr.2020.9.1.001
- Valbuena-Niño E. D., Peña D., Salinas D. V., and Chinchilla L. F. (2011). Modificación Superficial de un Acero AISI SAE 1045 mediante la implantación de iones de nitrógeno y titanio. *Revista Iteckne*, 8(1), 31-36. 10.15332/iteckne.v8i1.259
- Vasilescu, C., Drob, S. I., Calderón, J. M., Osiceanu, P., Popa, M. Vasilescu, E., and Marcu, M. (2015). Long-term corrosion resistance of new Ti-Ta-Zr alloy in simulated physiological fluids by electrochemical and surface analysis methods. *Corrosion Science*, 93, 310-323. 10.1016/j.corsci.2015.01.038
- Vladmir, I. K. and Tsygankov, P. A. (1997). The use of a high voltage discharge at low pressure for 3D ion implantation. *Surface and Coatings Technology*, 96(1), 68-74. 10.1016/S0257-8972(97)00117-5
- Voort, V., Lucas, G. M., and Manilova, E. P. (2004). Metallography and microstructures of stainless steels and maraging steels. *ASM Handbook: Metallography and Microstructures, International*, 9, 670-700. 10.31399/asm.hb.v09.a0003767
- Walsh, F. C., Ponce de León, C., Kerr, C., Court, S., and Barker, B. D. (2008). Electrochemical characterisation of the porosity and corrosion resistance of electrochemically deposited metal coatings. *Surface & Coatings Technology*, 202(21), 5092-5102. 10.1016/j.surfcoat.2008.05.008
- Was, G. S. (1990). Ion beam modification of metals: Compositional and microstructural changes. *Progress in Surface Science*, 32(3-4), 211-332. 10.1016/0079-6816(89)90005-1